16 Apr 1992

Calculation of Neutron Flux and Neutron Radiation Dose in a Human Phantom

L. Alan Smith

CALCULATION OF NEUTRON FLUX AND NEUTRON RADIATION DOSE IN A HUMAN PHANTOM

L. Alan Smith
Nuclear Engineering Department

ABSTRACT

At present, the neutron dose received by personnel working in nuclear installations is recorded by body surface dosimeters worn by workers. To estimate the true neutron dose to internal organs, this "surface dose" is multiplied by empirical factors to account for the attenuation of the body itself.

The objective of this work was to obtain better estimates of the internal dose by calculating the attenuation of the neutron flux provided by the body. Using DOT, a 2-D radiation transport code, the neutron flux as a function of energy was calculated at several points in a 2-D model of the human body. These flux values were used to calculate the neutron dose at all points in the human phantom. These neutron doses were then compared to the "surface dose." The ratios thus obtained could be used by practicing health physicists to evaluate internal doses.

INTRODUCTION

In every installation where neutrons may be present, accurate determination of the neutron dose received by personnel is of paramount importance. Currently, the neutron dose to internal organs of the body is calculated by multiplying the dose recorded by a surface dosimeter by an empirical factor. This factor accounts for changes in the neutron field caused by the body itself, which are important since the radiation dose from a neutron beam is very energy-dependent. DOT, a 2-D transport code, was used to calculate these factors in a human phantom.

CALCULATION

In order to preform neutron transport calculations, neutron cross sections are needed. These cross sections are calculated for different materials and energy groups from cross section libraries through the use of computer codes. In most cases, these codes collapse fine group cross sections into smaller broad group cross sections. The cross sections are collapsed because the computer time needed to run the codes is decreased if a smaller number of energy groups is utilized.

Computer Codes

Several computer codes were used for the calculation of the flux at points in the human phantom. The order in which these codes are used is outlined in Figure 1 on page 3. LAVA is used to setup the cross section library of isotopes in the model. The LAVA code reads these values from the BUGLE-80 collection which contains the cross sections of various materials collapsed to 47 neutron groups. Since the BUGLE-80 cross sections are contained in two different files, LAVA must be run twice if isotopes are needed from both files. NITAWL is used to combine the files created by the two LAVA runs. The created NITAWL cross section library is entered into the 1-D transport code, XSDRNPM. In XSDRNPM a 1-D model of the geometry to be studied, in this case the human body, is entered along with the neutron source position and energy spectrum. XSDRNPM calculates the flux as a function of position in the model and collapses the cross sections into a 20 broad group library from the original 47 groups of the BUGLE-80 library.

XSDRNPM creates the cross section library to be used in DOT, a 2-D transport code. In DOT, a 2-D model of the geometry under study is entered. As in XSDRNPM, the neutron source position and energy is set-up as desired. The neutron flux at several points of the model and at each of the 20 energy groups is calculated by DOT. These flux values can be used to calculate the neutron dose at positions inside the model relative to the surface dose.

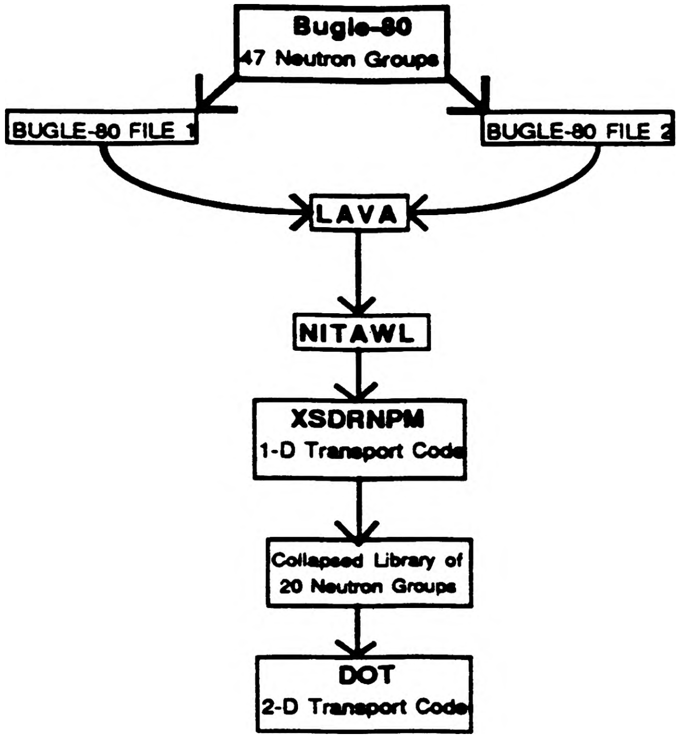

Figure 1. Computer Code Structure.

HUMAN PHANTOM

XSDRNPM

A 1-D model of the human waist line was used in XSDRNPM. The model is shown below in Figure 2. Slab geometry, S_8 angular quadrature, and P_3 scattering order were used for the calculation. Reflective boundaries were assumed on both sides of the model to simulate the containment area of a nuclear reactor. The fission spectrum of Uranium was used as the source on both sides. The 47 group cross sections from BUGLE-80 were collapsed to 20 groups. The energy groups and the resulting collapsed energy groups are shown in Table I on page 5.

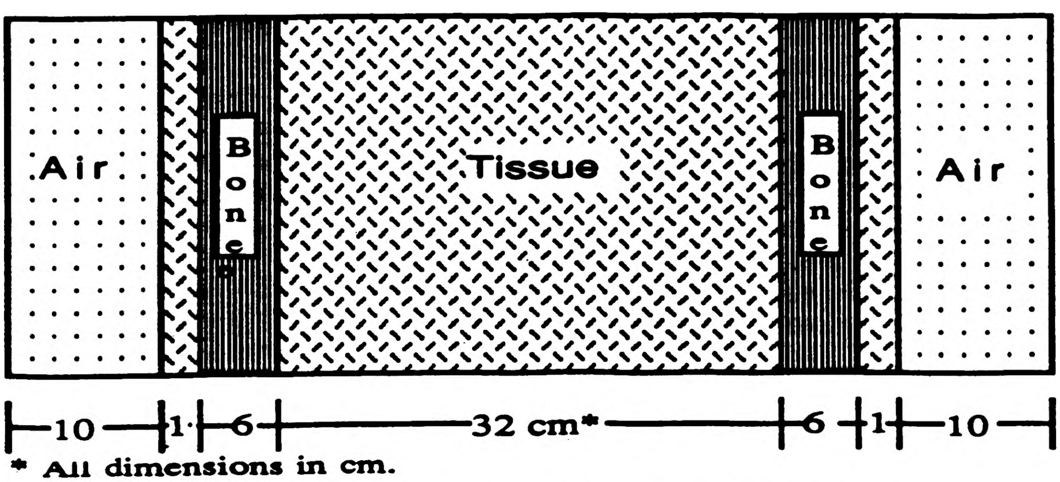

Figure 2. XSDRNPM 1-D Model of Human Waist.

Table I. Broad and Collapsed Energy Groups.

Fine Group Structure: Group No.	Fine Group Structure: Energy(MeV)	Broad Group Structure: Group No.	Broad Group Structure: Energy(MeV)
1	17.33299	1	17.33299
2	14.19100		
3	12.21400		
4	10.00000		
5	8.60100	2	8.6071
6	7.4682		
7	6.0653	3	6.0653
8	4.9659		
9	3.6788		
10	3.0119	4	3.0119
11	2.7253		
12	2.466		
13	2.3653		
14	2.3457	5	2.3457
15	2.2313		
16	1.9205		
17	1.653		
18	1.3534	6	1.3534
19	1.0026		
20	8.2080E-1		
21	7.4274E-1		
22	6.0810E-1	7	6.0810E-1
23	4.9798E-1		
24	3.6883E-1		
25	2.9720E-1		
26	1.8316E-1	8	1.8316E-1
27	1.1109E-1		
28	6.7379E-2		
29	4.0868E-2		
30	3.1828E-2	9	3.1828E-2
31	2.6058E-2		
32	2.4176E-2		
33	2.1875E-2	10	2.1875E-2
34	1.5034E-2		
35	7.1017E-3		
36	3.3546E-3	11	3.3546E-3
37	1.5846E-3		
38	4.5400E-4	12	4.5400E-4
39	2.1445E-4		
40	1.0130E-4	13	1.0130E-4
41	3.7267E-5	14	3.7267E-5
42	1.0677E-5	15	1.0677E-5
43	5.0435E-6	16	5.0435E-6
44	1.8554E-6	17	1.8554E-6
45	8.7642E-7	18	8.7642E-7
46	4.1399E-7	19	4.1399E-7
47	1.0000E-7	20	1.0000E-7
48	1.0000E-11	21	1.0000E-11

Three different materials were used in the model; general body tissue, bone tissue, and air. The weight percent of each isotope in these materials and the material's density are shown in Table II. The XSDRNPM code was used to produce the collapsed cross section library to be used in DOT and the 2-D model of the human body.

Table II. Weight Percent and Density of Isotopes Used in Model.

Isotope	General Tissue	Bone Tissue	Air
H	10.47%	7.04	0.00
C	23.02	22.80	0.00
N	2.34	3.90	78.94
O	63.21	48.60	21.06
Na	0.13	0.32	0.00
P*	0.84	17.35	0.00
Density (g/cm^3)	0.987	1.486	$1.29 \cdot 10^{-3}$

* Mg, Al, Si, S, Cl, K, Ca, and Fe isotopes were assumed to be P due to their small weight percent.

DOT

The 2-D model of the human body is shown in Figure 3 on page 6. X-Y geometry was used and reflective boundaries were assumed on the sides and the top of the model while the bottom of the model was assumed to be void. Two different neutron sources were considered; first, the fission spectrum and second, a source of only 0.5 MeV neutrons. The source was placed in the air surrounding the phantom. A XSDRNPM model of a typical containment area was run in XSDRNPM to try to determine a neutron spectrum with an <u>average</u> energy of 0.5 MeV. However, the spectrum calculated by the model did not have the desired average energy and could not be used in DOT. Therefore, the source containing only 0.5 MeV neutrons was used.

A 2-D model of the torso region was examined in R-Θ geometry too. The model used is shown in Figure 4. The same neutron sources were used as in the X-Y geometry model.

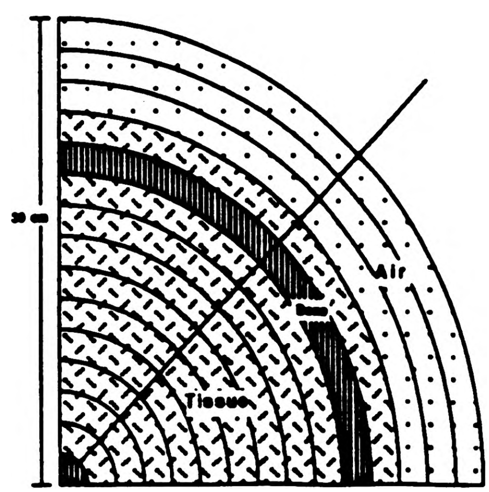

Figure 4. Model of Chest Area in R-Θ Geometry.

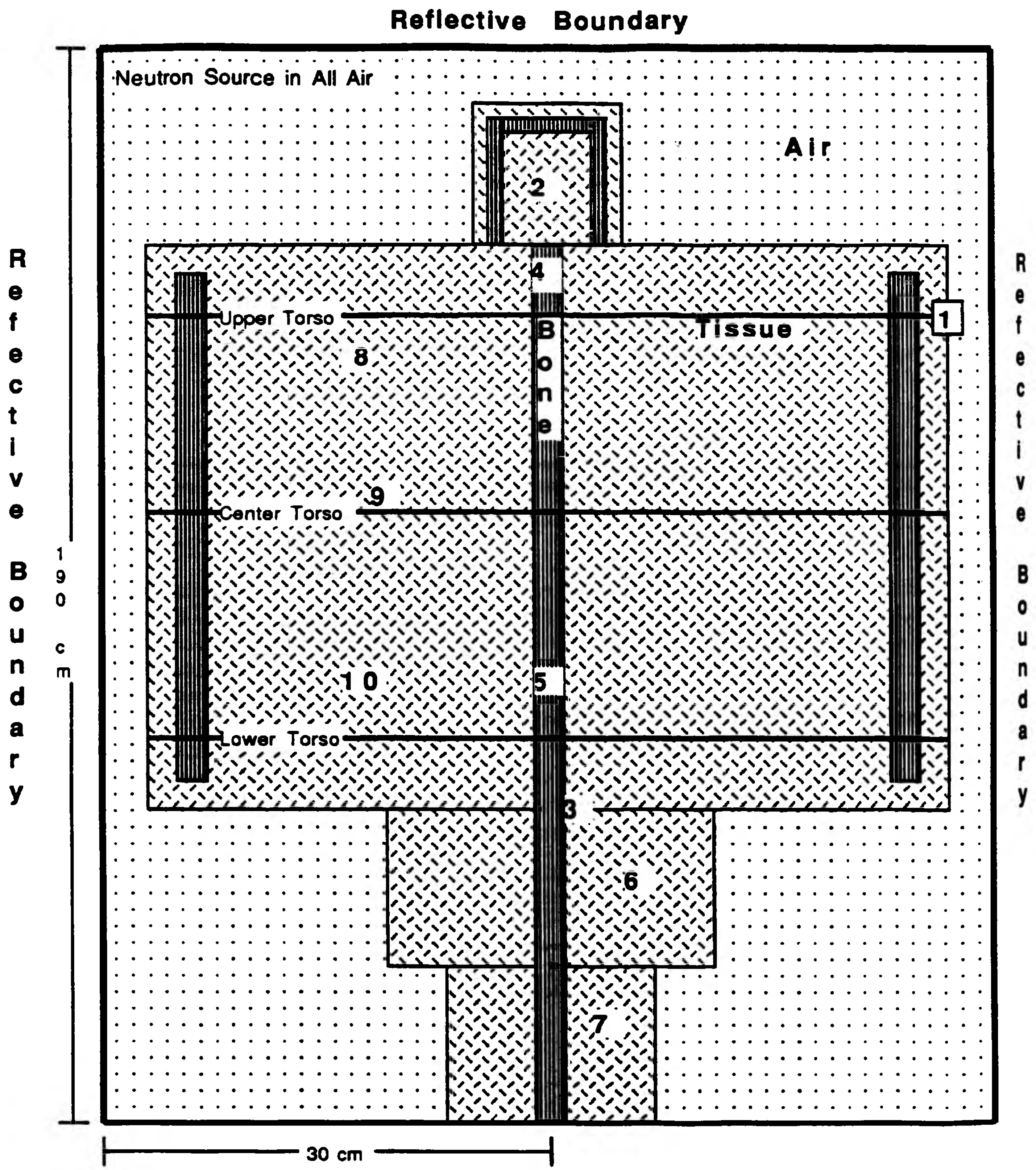

Figure 3. 2-D Model of Human Phantom.

NEUTRON DOSE

After the neutron fluxes were calculated by DOT, these fluxes were utilized in the calculation of the neutron dose at several points in the phantom. The fluxes were converted to radiation doses through the use of two different formulas. The American National Standard is the source of the flux-to-dose-rate conversion factors at different neutron energies. The first dose calculation used the 1990 version of the formula whereas 1977 conversion factors were used in the second calculation. These dose equations and there coefficients are shown in Table III.

Table III. Neutron Flux-To-Dose-Rate Conversion Factors.

Equation 1-1977 Version

Polynomial Coefficients In Analytic Fit-- $\ln DF(E) = A+B*X+C*X^2+D*X^3$.
$DF(E) = (rem/hr)/(n/cm^2\text{-}s)$, E=neutron energy in MeV, and X=Ln E.

Neutron Energy (MeV)		A	B	C	D
2.5 -08	to 1.0-07	-1.2514+01			
1.0 -07	to 1.0-02	-1.2210+01	1.7165-01	2.603402	1.0273 -03
0.01	to 0.1	-8.9302	7.8440-01		
0.1	to 0.5	-8.6632	9.0037-01		
0.5	to 1.0	-8.9359	5.0696-01		
1.0	to 2.5	-8.9359	-5.5979-02		
2.5	to 5.0	-9.2822	3.2193-01		
5.0	to 7.0	-8.4741	-1.8018-01		
7.0	to 10.0	-8.8247			
10.0	to 14.0	-1.1208+01	1.0352		
14.0	to 20.0	-9.1202	2.4395-01		

Equation 2-1990 Version

Polynomial Coefficients in Analytic Fit-
$h(E)=10^{-12}*EXP(A+B*X+C*X^2+D*X^3+E*X^4)$ $Sv\text{-}cm^2$, E=Energy (MeV), and X=Ln E.

Neutron Energy Bounds	A	B	C	D	E
E<=0.01 MeV	2.42866	0.65022	0.08819	0.00475	0.00009
E>0.01MeV	4.22421	0.84705	-0.06771	-0.01213	0.00183

These doses were then divided by a reference "surface dose" which would have been read by a dosimeter on the phantom's chest to produce a relative dose. The dose just inside the body was much lower than that of the air just outside the body; therefore, all doses were divided by the average of these two doses to attain the reference "surface dose". The relative doses at several points of the body are shown in Table IV. The 1977 equation consistently gives lower dose rates for both energies. Figure 5 on page 8 shows the difference between the dose rates at the center of the torso for both dose equations. The difference between the two dose equations is greater for the 0.5 MeV spectrum. The dose at the center waist line of the phantom is about 4% of the dose

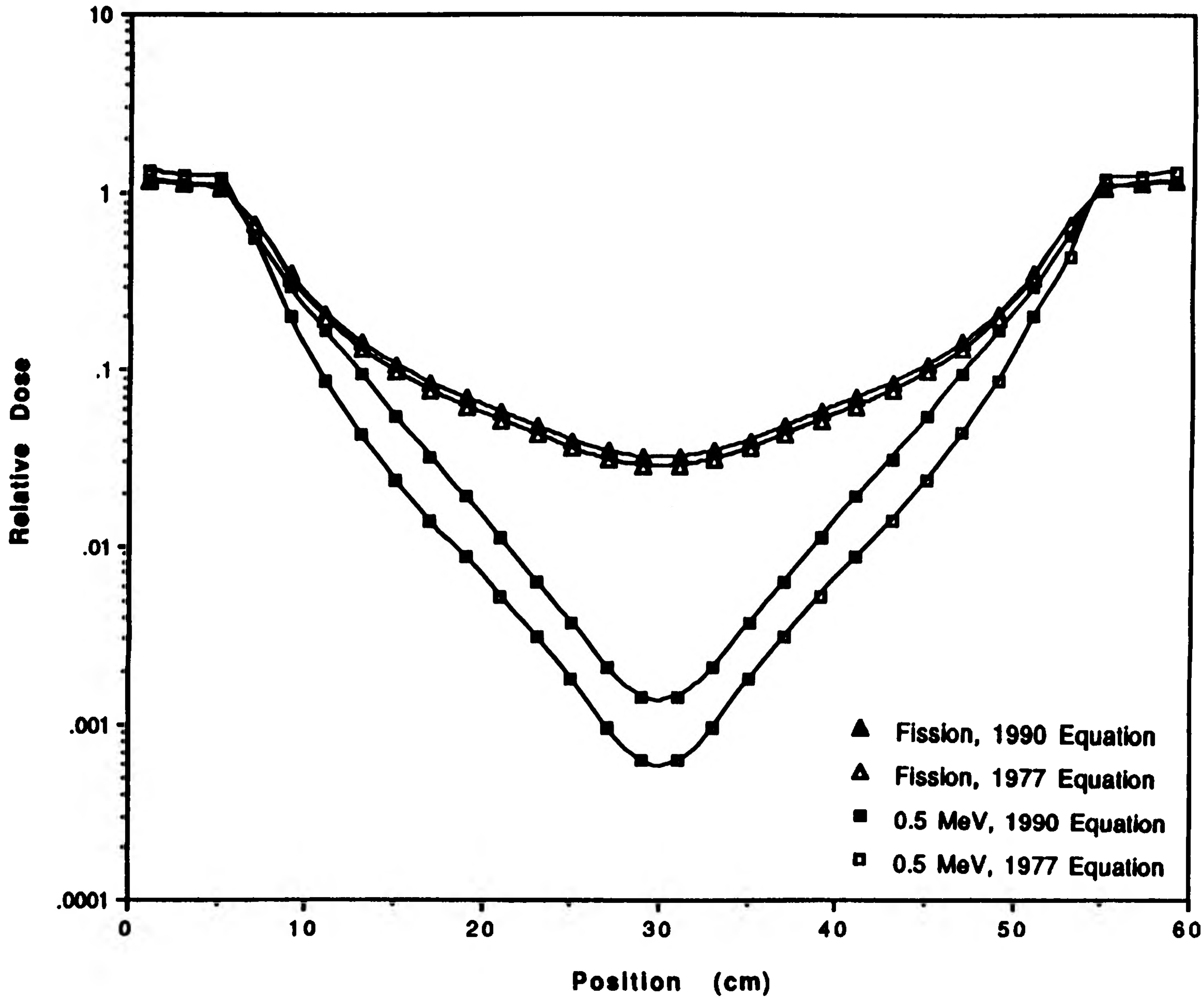

Figure 5. Relative Dose vs. Position at Waist Line Comparing 1990 and 1977 Dose Equations.

Table IV. Relative Dose Percent at Several Points in Phantom.

Position	Uranium Fission Spectrum 1977 Equation	Uranium Fission Spectrum 1990 Equation	0.5 MeV Neutrons 1977 Equation	0.5 MeV Neutrons 1990 Equation
Surface or pocket dosimeter position(1*)	1.00	1.00	1.00	1.00
Head(2)	0.30	0.33	0.13	0.46
Pelvic Region(3)	0.07	0.08	0.002	0.007
Upper Spine(4)	0.07	0.08	0.007	0.002
Lower Spine(5)	0.03	0.032	1.37E-4	4.61E-4
Upper Leg(6)	0.32	0.34	0.08	0.21
Lower Leg(7)	0.51	0.53	0.26	0.42
Mid-Region(8)	0.05	0.06	3.45E-5	7.11E-5
Mid-Region(9)	0.03	0.04	1.52E-4	5.26E-4
Mid-Region(10)	0.02	0.05	0.001	0.005

*Number corresponds to Figure 3 on page 6.

received at the surface for the fission spectrum source and only 0.1% for the 0.5 MeV source. This drop in dose is caused by the decrease in the neutron energy and flux as neutrons pass through the body.

The dose at the middle of the torso was calculated in X-Y and R-Θ geometry. Figures 6 and 7 on pages 10 and 11 show the relationship between the dose rate calculated in the X-Y and R-Θ geometries in DOT. In the X-Y geometry, three cross sections were examined; the upper, center, and lower torso as shown in Figure 3. The center-line of the model was used in the R-Θ geometry. In Figure 6 the source is the fission spectrum, while Figure 7 the 0.5 MeV source is examined. The R-Θ geometry matches X-Y geometry well for the fission spectrum especially at the upper and lower lines of the torso. It does not match as well of the 0.5 MeV source, however. The relationship between the dose at different cross sections for the two sources is shown in Figure 8 on page 12. The dose due to the 0.5 MeV source is lower than that of the fission source at all positions. The difference in the dose at the center of the torso is larger than that of the upper and lower torso.

CONCLUSION

Since, at the present time, it is impossible to measure the dose received by internal organs, empirical factors must be used to estimate the doses received by these organs. Using a computer model of a human body, the dose to these organs can be calculated by somewhat reliable transport codes such as XSDRNPM and DOT. The radiation dose relative to the "surface dose" that would be measured by a dosimeter was found at several places in the human phantom. These factors can be used to estimate the dose to internal organs when the "surface dose" is known.

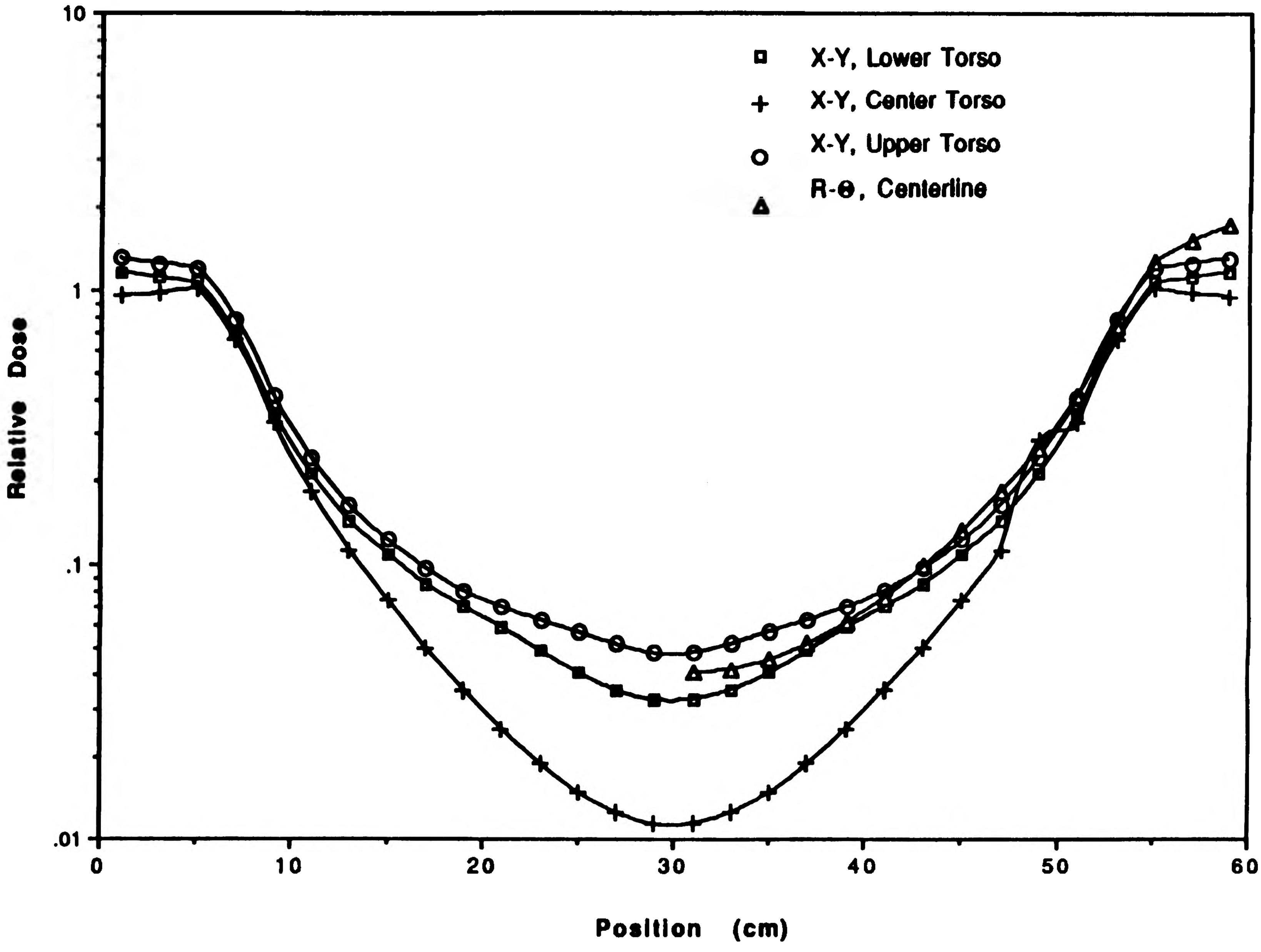

Figure 6. Dose vs. Position for R-O and X-Y Model for Fission Spectrum.

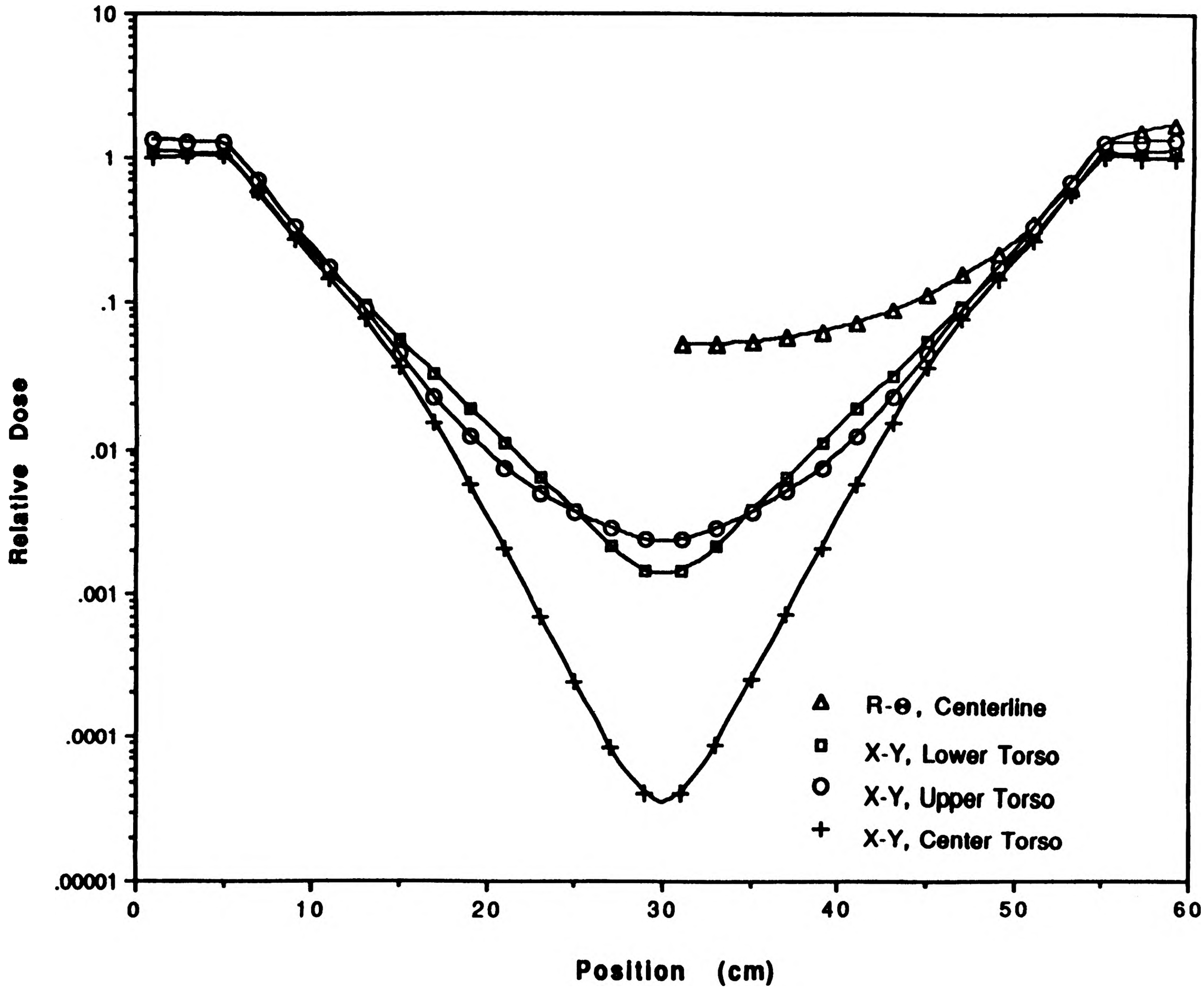

Figure 7. Dose vs. Position for R-O and X-Y Model for 0.5 MeV Spectrum.

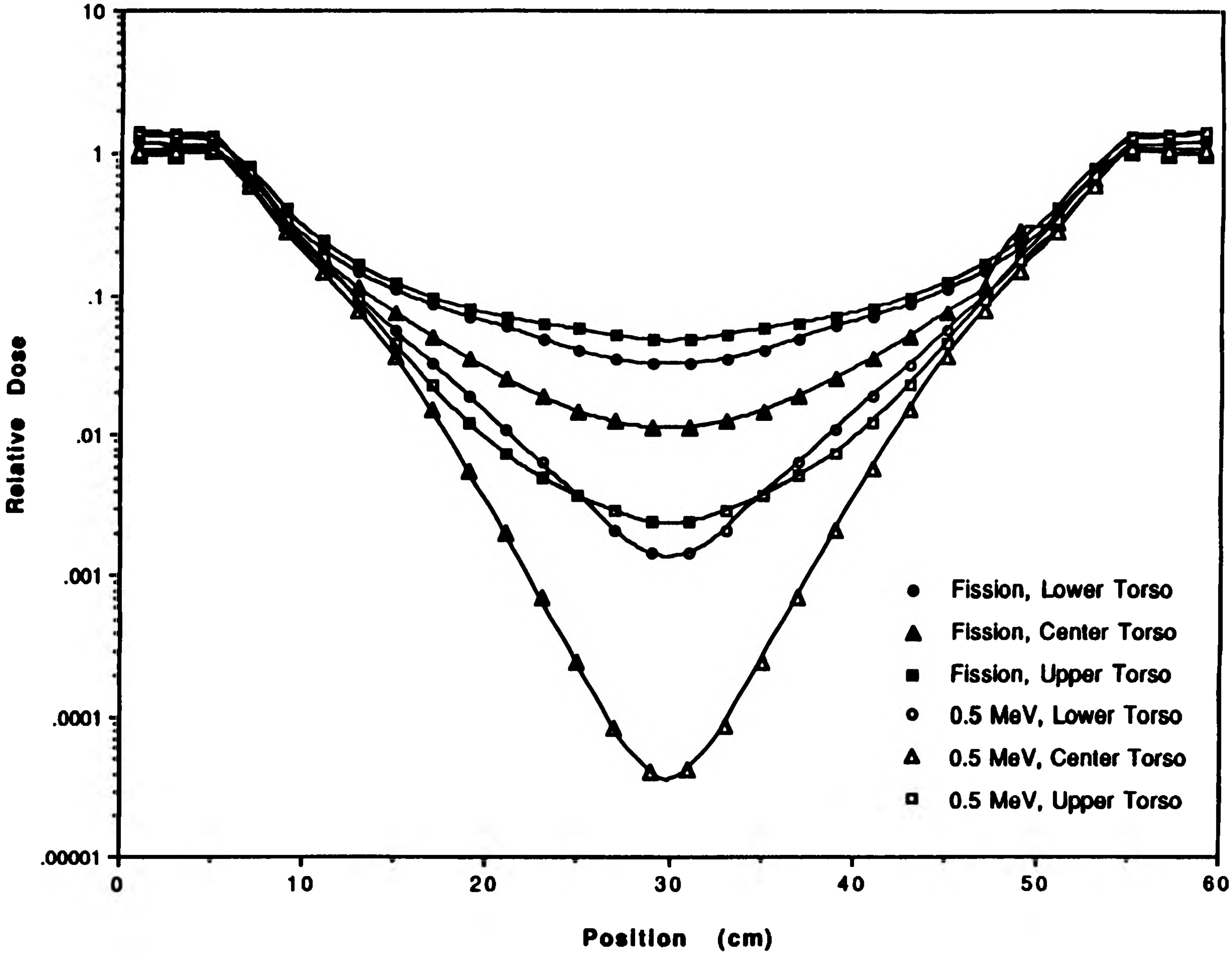

Figure 8. Dose vs. Position for Fission and 0.5 MeV Spectra.